Surface optical phonons in a triaxial ellipsoidal quantum dot

O. Reese and L. C. Lew Yan Voon
Department of Physics, Worcester Polytechnic Institute, 100 Institute Road, Worcester, Massachusetts 01609, USA

M. Willatzen
Mads Clausen Institute, University of Southern Denmark, Grundtvigs Allé 150, DK-6400 Sønderborg, Denmark
(Received 4 December 2003; revised manuscript received 14 May 2004; published 3 August 2004)

The surface optical phonon eigenmodes in ellipsoidal quantum dots were calculated using the dielectric-continuum model. The problem is exactly solvable in terms of ellipsoidal coordinates and the eigenmodes are written in terms of Lamé polynomials. A study of the mode frequency dependence on the shape of the dots is carried out. This represents a generalization over earlier work on spheres and spheroids. Differences in the results obtained using an optically active and an optically passive host is presented. The size independence of the mode frequencies for a quantum dot of arbitrary shape is proven.

DOI: 10.1103/PhysRevB.70.075401 PACS number(s): 63.22.+m

I. INTRODUCTION

In a three-dimensional, periodic ionic crystal, it is known that, in the long-wavelength limit, there are transverse optical (TO) and longitudinal optical (LO) phonon modes, with the LO phonon at a higher energy. It was later established that, in a finite crystal, surface optical (SO) modes also appear in addition to the confined bulk modes. While there were earlier results, the most convincing calculation was probably the work of Fuchs and Kliewer[1] on a finite slab. An excellent review of the early works was provided by Ruppin and Englman.[2]

The simplest treatment that works in the long-wavelength limit is the so-called continuum electrostatics[2] or dielectric-continuum model (DCM), whereby the optical vibrational modes are treated in terms of the associated electrostatic fields (solutions of the Laplace equation) and subject to electrostatic boundary conditions. There are limitations to the model (such as consideration of mechanical boundary conditions) but it has been shown to be appropriate for certain physical properties such as frequencies,[3] and will therefore be used here without further justification. Retardation effects (polaritons) will also not be considered here. Long-range Coulomb forces in ionic crystals make the solutions shape and size dependent in general. A description of this in terms of curvilinear coordinates was given by Englman and Ruppin.[4] This was found to be the case for finite rectangular slabs and circular cylinders;[5] a comparison between theory and Raman-scattering experiment of modes in the latter case was recently achieved.[6] However, they also found that the eigenfrequencies for spherical crystals are size independent.[4,5] It is known that the only three-dimensional shapes [quantum dot (QD)] that can be solved exactly have one-coordinate surfaces[4] (spheres, spheroids, and ellipsoids) and variations thereof (such as a shell structure).[4,5] The spherical dot was solved by Englman and Ruppin.[4,5] The spheroidal dot has also been studied;[7,8] however, one work used an optically active host while the other used an optically passive one. The motivation for the latter study was the widespread growth of QDs and the fact that an attempted growth of a spherical dot might often result in a nonspherical shape. It was reported that the size independence of the eigenfrequencies for the sphere did not carry over to the spheroid[8,9] though we will show this to be incorrect.

In this paper, we extend earlier work on spheres and spheroids to triaxial ellipsoids. For practical applications this is essential since even a spheroid might not represent all the "spherical" QD's being grown. An ellipsoid is the simplest region bounded by a one-coordinate surface that reduces to a spheroid and a sphere. It is also the last unsolved simple shape. We are particularly interested in the shape dependence of the SO mode frequencies and in the difference between using models of an optically active and of an optically passive host. In the process, we have also established the size independence of the problem.

II. THEORY

A. Dielectric continuum model

We first present a summary of the DCM. The model is applied to a QD of isotropic dielectric material embedded in an infinite-volumed dielectric host material. We will first treat the host as optically inactive (i.e., with a constant dielectric constant); this is appropriate for isolated QDs. We will then show how to account for optically active hosts; this problem for other shapes was studied by Knipp and Reinecke.[7,10] Treating the host as optically active will lead to additional barrier-like SO modes (where the frequencies fall within the rest-strahl region of the barrier material). In the DCM, we start with the standard electrostatic equations in the absence of free charges

$$\nabla \cdot \mathbf{D} = 0, \tag{1}$$

$$\mathbf{E} = -\nabla \phi(\mathbf{r}), \tag{2}$$

where $\mathbf{D}$ is the electric displacement, $\mathbf{E}$ is the electric field, and ϕ is the scalar potential. The fields originate from the relative displacement of the ions in a unit cell. The constitutive relation gives

$$\mathbf{D} = \epsilon_0 \epsilon(\omega)\mathbf{E}, \tag{3}$$

where $\epsilon(\omega)$ is the polariton dielectric function[11]

$$\epsilon(\omega) = \epsilon(\infty)\frac{\omega^2 - \omega_{\mathrm{LO}}^2}{\omega^2 - \omega_{\mathrm{TO}}^2}, \tag{4}$$

where $\epsilon(\infty)$ is the so-called high-frequency dielectric constant due to electronic polarization and ω_{LO} (ω_{TO}) is the LO (TO) long-wavelength (angular) frequency. Putting Eqs. (1)–(3) together gives

$$\epsilon(\omega)\nabla^2\phi = 0. \tag{5}$$

The solution

$$\epsilon(\omega) = 0, \tag{6}$$

leads to bulk-like confined LO phonons. The solution

$$\nabla^2\phi = 0, \tag{7}$$

gives the SO phonon modes. By applying the boundary conditions of continuity of $\mathbf{E}_{\parallel}$ and $\mathbf{D}_{\perp}$ at the interfaces between the two media, one can solve for the eigenfrequencies.

B. Scale invariance

There has been some confusion in the literature about the size dependence or not of the SO phonon mode frequencies.[4,5,7,9] Thus, Englman and Ruppin[4] referred to a size and shape dependence, they found a size dependence (on the cylinder radius) for a cylindrical wire[5] but not for a sphere, and Comas *et al.*[9] recently reported that the mode frequencies for spheroids do depend on size. On the other hand, Knipp and Reinecke[7] had advanced that there is a size independence for any shape due solely to the long range nature of the Coulomb force.

In fact, the size independence can be mathematically derived for any three-dimensional shape using the Laplace equation, together with the electromagnetic boundary conditions. To wit, if one rescales the coordinates $\mathbf{r} = \alpha\mathbf{r}'$, the Laplace equation is invariant

$$\nabla'^2\phi(\alpha\mathbf{r}') = 0.$$

The size dependence reported for wires can be explained by the fact that one is only scaling two of the three coordinates. This can also be seen explicitly by noting that the potential field, as a function of only the x and y coordinates (with z along the wire axis), no longer satisfies the Laplace equation; rather, it now satisfies a Helmholtz equation[10]

$$\nabla_{x,y}^2\phi(x,y) - k^2\phi(x,y) = 0, \tag{8}$$

where $\phi(\mathbf{r}) = \phi(x,y)e^{ikz}$. Rescaling x and y (e.g., $x = Rx'$, $y = Ry'$) requires a rescaling of the wave number as well ($k' = kR$) in order to maintain the invariance of the Helmholtz equation. The apparent size dependence for spheroids reported by Comas *et al.*[9] is incorrect and will be clarified latter.

III. LAPLACE'S EQUATION IN ELLIPSOIDAL COORDINATES

A. Ellipsoidal coordinates

The problem is exactly solvable if one uses ellipsoidal coordinates. The ellipsoidal coordinate system is one of the most general orthogonal curvilinear coordinate systems; indeed, it degenerates into the ten other systems the Laplace equation is simply separable in Refs. 12 and 13. It is related to the Cartesian coordinates in the following manner:

$$x = \frac{(\xi_1^2 - a^2)^{1/2}(\xi_2^2 - a^2)^{1/2}(\xi_3^2 - a^2)^{1/2}}{(a^2 - c^2)^{1/2}(a^2 - b^2)^{1/2}},$$

$$y = \frac{(\xi_1^2 - b^2)^{1/2}(\xi_2^2 - b^2)^{1/2}(\xi_3^2 - b^2)^{1/2}}{(b^2 - c^2)^{1/2}(b^2 - a^2)^{1/2}},$$

$$z = \frac{(\xi_1^2 - c^2)^{1/2}(\xi_2^2 - c^2)^{1/2}(\xi_3^2 - c^2)^{1/2}}{(a^2 - c^2)^{1/2}(b^2 - c^2)^{1/2}}, \tag{9}$$

with

$$\xi_1 > a > \xi_2 > b > \xi_3 > c. \tag{10}$$

One set of ξ_1, ξ_2, ξ_3 corresponds to eight cartesian points. In general, a, b, c can take on any values subject to the convention given in Eq. (10). It turns out the values are fixed when space is partitioned by an ellipsoid. Thus, let the cartesian coordinates of the points of intersection of the ellipsoid with the cartesian axes be $\pm x_0, \pm y_0, \pm z_0$. Then

$$(\xi_0^2 - a^2)^{1/2} = x_0,$$

$$(\xi_0^2 - b^2)^{1/2} = y_0,$$

$$(\xi_0^2 - c^2)^{1/2} = z_0, \tag{11}$$

where ξ_0 is the value of ξ_1 on the ellipsoidal surface (recall that ξ_1 alone defines an ellipsoidal surface). We observe that the ordering $a > b > c$ implies $z_0 > y_0 > x_0$. There are four unknowns on the left-hand side of Eqs. (11), three constants given on the right-hand side. We, therefore, have the freedom to set one of the unknowns; we choose $c = 0$ as is commonly done.[12]

When comparing this coordinate system to the spherical system, the ξ_1 variable can be described as the radial component while ξ_2 and ξ_3 are the angular components. Thus, the volume of an ellipsoid with $\xi_1 = \xi_0$ has the simple form

$$V_{\mathrm{ellipse}} = \frac{4\pi}{3}\xi_0\sqrt{\xi_0^2 - a^2}\sqrt{\xi_0^2 - b^2}. \tag{12}$$

B. Separation of Laplace's equation

Laplace's equation is separable in this coordinate system yielding three identical ordinary differential equations. Let

$$\phi(\xi_1, \xi_2, \xi_3) = X_1(\xi_1)X_2(\xi_2)X_3(\xi_3), \tag{13}$$

then we have[12–15]

$$\frac{d^2X_i}{d\xi_i^2} + \left[\frac{\xi_i}{(\xi_i^2-a^2)} + \frac{\xi_i}{(\xi_i^2-b^2)}\right]\frac{dX_i}{d\xi_i} + \left[\frac{-m(m+1)\xi_i^2+q}{(\xi_i^2-a^2)(\xi_i^2-b^2)}\right]X_i = 0, \tag{14}$$

for $i=1,2,3$. This is known as Lamé's equation. Note that we have three equations, each with its own domain. The equations have regular singular points at $\xi_i=\pm b, \pm a, \infty$. Nevertheless, they share the same two separation constants m and q. Thus, all three solutions must be well behaved for given m and q. This implies we need solutions well behaved for the whole domain $0<\xi_i<\infty$.

C. Series solutions

The solutions of these equations can be expressed as a series expansion.[12] There are three ways of developing a series solution. One is to set (with z standing for one of ξ_1, ξ_2, ξ_3):

$$X(z) = \sum_n d_n z^n. \tag{15}$$

Another possible solution is of the form

$$X(z) = \sqrt{z^2-a^2}B(z) \quad \text{or} \quad \sqrt{z^2-b^2}B(z), \tag{16}$$

where $B(z)$ is a series function. Yet another is

$$X(z) = \sqrt{z^2-a^2}\sqrt{z^2-b^2}B(z). \tag{17}$$

Since they lead to different recurrence relations, we do not list the latter here. The infinite series expansions converge up to the nearest singularity, either $z=a$ or $z=b$. However, if m is chosen to be an integer and if q has a polynomial relation to a and b then we may obtain polynomial solutions which are convergent up to infinity. It is these solutions, known as Lamé polynomials (E_m^p) and the related polynomials of the second kind (F_m^p), which are of primary interest. For each m value, there are $(2m+1)$ p values. Indeed, in the limit of large ξ_0, the ellipsoid approaches a sphere of radius $r\sim\xi_0$, and m becomes the separation constant l in spherical polar coordinates. A few of the lowest functions are shown in Fig. 1. The full solution to Laplace's equation is then a product of the Lamé polynomials known as ellipsoidal harmonics. Due to the requirement for finiteness of the three polynomials simultaneously, the product function consists of the same three Lamé polynomials.

IV. SO PHONON MODES

The electrostatic potential for a SO mode is given by

$$\phi = \begin{cases} A_m^p E_m^p(\xi_1)E_m^p(\xi_2)E_m^p(\xi_3) & \xi_1 \leqslant \xi_0, \\ B_m^p F_m^p(\xi_1)E_m^p(\xi_2)E_m^p(\xi_3) & \xi_1 > \xi_0. \end{cases} \tag{18}$$

For both ϕ and $E_\parallel$ to be continuous at the boundary, the constant B_m^p must satisfy

$$B_m^p = A_m^p \frac{E_m^p(\xi_0)}{F_m^p(\xi_0)}. \tag{19}$$

Now we solve for the boundary condition on $D_\perp$, giving

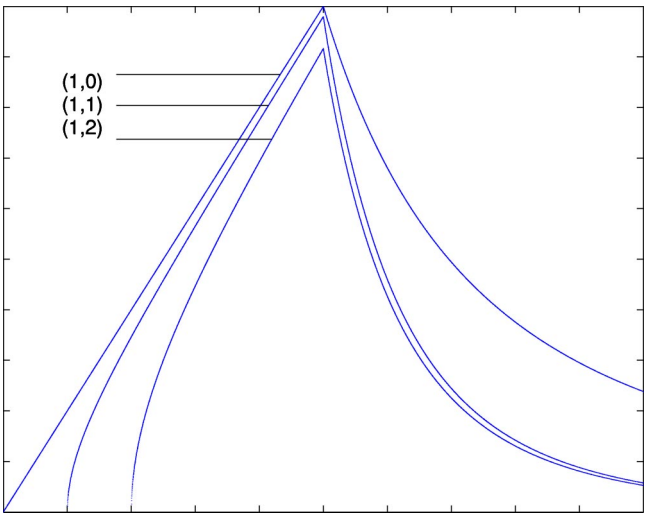

FIG. 1. A few Lamé functions both inside and outside an ellipsoid: $(m,p)=(1,0),(1,1),(1,2)$.

$$A_m^p \epsilon_1 E_m^{p\prime}(\xi_0) = A_m^p \epsilon_2 \frac{E_m^p(\xi_0)}{F_m^p(\xi_0)} F_m^{p\prime}(\xi_0), \tag{20}$$

where ϵ_1 (ϵ_2) is the dielectric function inside (outside) the ellipsoid. Rewriting this equation gives

$$\frac{\epsilon_1}{\epsilon_2} = \frac{E_m^p(\xi_0)F_m^{p\prime}(\xi_0)}{E_m^{p\prime}(\xi_0)F_m^p(\xi_0)} \equiv f_{mp}(\xi_0). \tag{21}$$

Note that the right-hand side of Eq. (21) is only a function of the shape and size of the QD, and not on the model for the dielectric functions. If we make the substitution $\epsilon_2=\epsilon_D$, the dielectric function of the surrounding medium, and $\epsilon_1=\epsilon_1(\omega_{mp})$, then by using the boundary condition on $D_\perp$ and Eq. (4), one arrives at

$$\frac{\omega_{mp}^2}{\omega_{\mathrm{TO}}^2} = \frac{\epsilon(0)-\epsilon_D f_{mp}(\xi_0)}{\epsilon(\infty)-\epsilon_D f_{mp}(\xi_0)}. \tag{22}$$

This relation defines the allowed modes of vibration in terms of the shape and size of the QD, in agreement with a similar relation found for quantum dots with oblate and prolate spheroidal geometries.[9] It should be noted that unlike the case of the spherical dot, and similar to the case of the prolate/oblate spheroid, the parameter ξ_0 of the QD is a determining factor in solving for the allowed frequencies. Indeed, this has led Comas and co-workers[9] to mistakenly claim that the frequencies are size dependent for spheroids (their Figs. 1 and 2). However, changing ξ_0 changes not just the size but also the shape; an ellipsoid becomes more spherical as ξ_0 increases [see Eq. (9)] and similar considerations apply to the case of the spheroid. Their plots of mode frequencies versus ξ_0 (their Figs. 1 and 2) is, therefore, not an indication of size dependence but rather shape dependence. Thus, the explicit dependence on ξ_0 in Eq. (22) must be properly interpreted. As a check we have carried out numerical calculations (using parameters reported in the next subsection) for the ellipsoid whereby ξ_0 was changed but the shape was kept constant (this is possible for the ellipsoid by changing the b/a ratio

simultaneously) and we found no change in the mode frequencies.

It is expected that, at large radial values, the allowed frequencies of an ellipsoid should converge to those of the spherical case. If we take the $\lim_{\xi_0\to\infty} f_{mp}(\xi_0)$:

$$\lim_{\xi_0\to\infty}\frac{E_m^p(\xi_0)F_m'^p(\xi_0)}{E_m^{p\prime}(\xi_0)F_m^p(\xi_0)}=\frac{\xi_0^{\,m}}{m\xi_0^{\,m-1}}\frac{-(m+1)\xi_0^{\,-m-2}}{\xi_0^{\,-m-1}}=-\frac{m+1}{m}. \tag{23}$$

Using this in Eq. (22), we get the same solution as the spherical QD. Moreover, just like the spherical QD, the allowed frequencies are dependant upon one separation constant (m):

$$\frac{\omega_{mp}^2}{\omega_{TO}^2}=\frac{m\epsilon(0)+(m+1)\epsilon_D}{m\epsilon(\infty)+(m+1)\epsilon_D}. \tag{24}$$

Looking further at the results of the sphere, we see that there is a theoretical minimum and maximum

$$\lim_{m\to 0}\frac{m\epsilon(0)+(m+1)\epsilon_D}{m\epsilon(\infty)+(m+1)\epsilon_D}=1, \tag{25}$$

$$\lim_{m\to\infty}\frac{m\epsilon(0)+(m+1)\epsilon_D}{m\epsilon(\infty)+(m+1)\epsilon_D}=\frac{\epsilon(0)+\epsilon_D}{\epsilon(\infty)+\epsilon_D}. \tag{26}$$

This implies that the ellipsoid must also be bound by the same frequencies in the limit $\xi_0\to\infty$. What is more, both the prolate spheroid and the oblate spheroid frequencies are bound by these same two limits.[9]

For an optically active host, the SO mode frequencies are given by

$$\omega_{mp}^2=\frac{-(\tilde{\omega}_{\rm LO}^2+\tilde{\omega}_{\rm TO}^2)\pm\sqrt{(\tilde{\omega}_{\rm LO}^2+\tilde{\omega}_{\rm TO}^2)^2-4(\epsilon'-f_{mp})(\omega_{\rm LO,1}^2\omega_{\rm TO,2}^2\epsilon'-f_{mp}\omega_{\rm LO,2}^2\omega_{\rm TO,1}^2)}}{2(\epsilon'-f_{mp})}, \tag{27}$$

where

$$\tilde{\omega}_{\rm LO}^2=\omega_{\rm LO,2}^2 f_{mp}-\epsilon'\omega_{\rm LO,1}^2,\quad \tilde{\omega}_{\rm TO}^2=\omega_{\rm TO,1}^2 f_{mp}-\epsilon'\omega_{\rm TO,2}^2, \tag{28}$$

$$\epsilon'=\frac{\epsilon_1(\infty)}{\epsilon_2(\infty)}.$$

V. CALCULATIONS

We carried out explicit calculations to investigate the shape dependence of the eigenfrequencies. For concreteness, we consider a GaAs QD embedded in an AlAs host. The parameters needed were taken from Knipp and Reinecke:[7] $\omega_{\rm LO,1}=292\ {\rm cm}^{-1}$, $\omega_{\rm TO,1}=268\ {\rm cm}^{-1}$, $\epsilon_1(\infty)=10.89$, $\omega_{\rm LO,2}=404\ {\rm cm}^{-1}$, $\omega_{\rm TO,2}=362\ {\rm cm}^{-1}$, $\epsilon_2(\infty)=8.16$. The nonoverlapping reststrahl regions of the two materials leads to distinct dot-like and barrier-like interface modes where the frequencies fall within the reststrahl region of the appropriate material.[7]

The lowest mode has $(m,p)=(0,0)$. This corresponds to a constant potential inside the dot and, therefore, no electric field inside ($E_0^{0\prime}=0$). Equation (20) becomes

$$\epsilon_2 E_0^0(\xi_0)F_0^0(\xi_0)'=0. \tag{29}$$

Now[12]

$$F_0^0(\xi_1)=\int_{\xi_1}^{\infty}\frac{dx}{\sqrt{(x^2-a^2)(x^2-b^2)}}=\frac{1}{a}{\rm sn}^{-1}\left(\frac{a}{\xi_1},\frac{b}{a}\right).$$

Thus, $F_0^0(\xi_1)'$ has no zeroes and Eq. (29) requires $\epsilon_2=0$. This cannot happen for a passive dielectric outside the QD and, therefore, the $(0,0)$ mode is absent in such a case. For an optically active dielectric outside, the mode is allowed and has frequency $\omega_{\rm LO,2}$. Our result for the ellipsoid is consistent with earlier results for the sphere.[2,7] For an isolated sphere or one embedded in a passive dielectric, the $l=0$ mode does not exist. With an optically active dielectric outside, the electric field of the $l=0$ mode falls as $1/r^2$, which is the same behaviour as for $F_0^0(\xi_1)'$ for large ξ_1.

The shape dependence of all the three $(1,p)$ modes are given in Fig. 2. The twofold (threefold) degeneracy of the spheroid (sphere) is lifted but, more importantly, the shape dependence is in general different. Inside the QD, the lowest mode, with $(m,p)=(1,0)$, can be written as

$$\phi_1^0\sim E_1^0(\xi_1)E_1^0(\xi_2)E_1^0(\xi_3)=abz. \tag{30}$$

It is known in the literature as an ellipsoidal harmonic of the second species.[12] The electric field only has a z component which is constant inside the QD but decaying outside. Results for the eigenfrequencies are shown in Fig. 2 for both the optically active (left and middle panels) and optically passive (right panel) hosts. The frequency is plotted as a function of the fractional difference between the smallest minor axis and the major axis

$$\frac{x_0}{z_0}=\frac{\sqrt{\xi_1^2-a^2}}{\xi_1}=\alpha. \tag{31}$$

In the calculations, ξ_1 is kept constant at 100 and α decreased (from right to left in Fig. 2). The effect is equivalent to leaving a constant and increasing ξ_1 (which would make the ellipsoid more spheroidal). This leads to one of the curves in the figure for a given b value. Also, all the spheroidal limits lead to prolate spheroids. On the same figure,

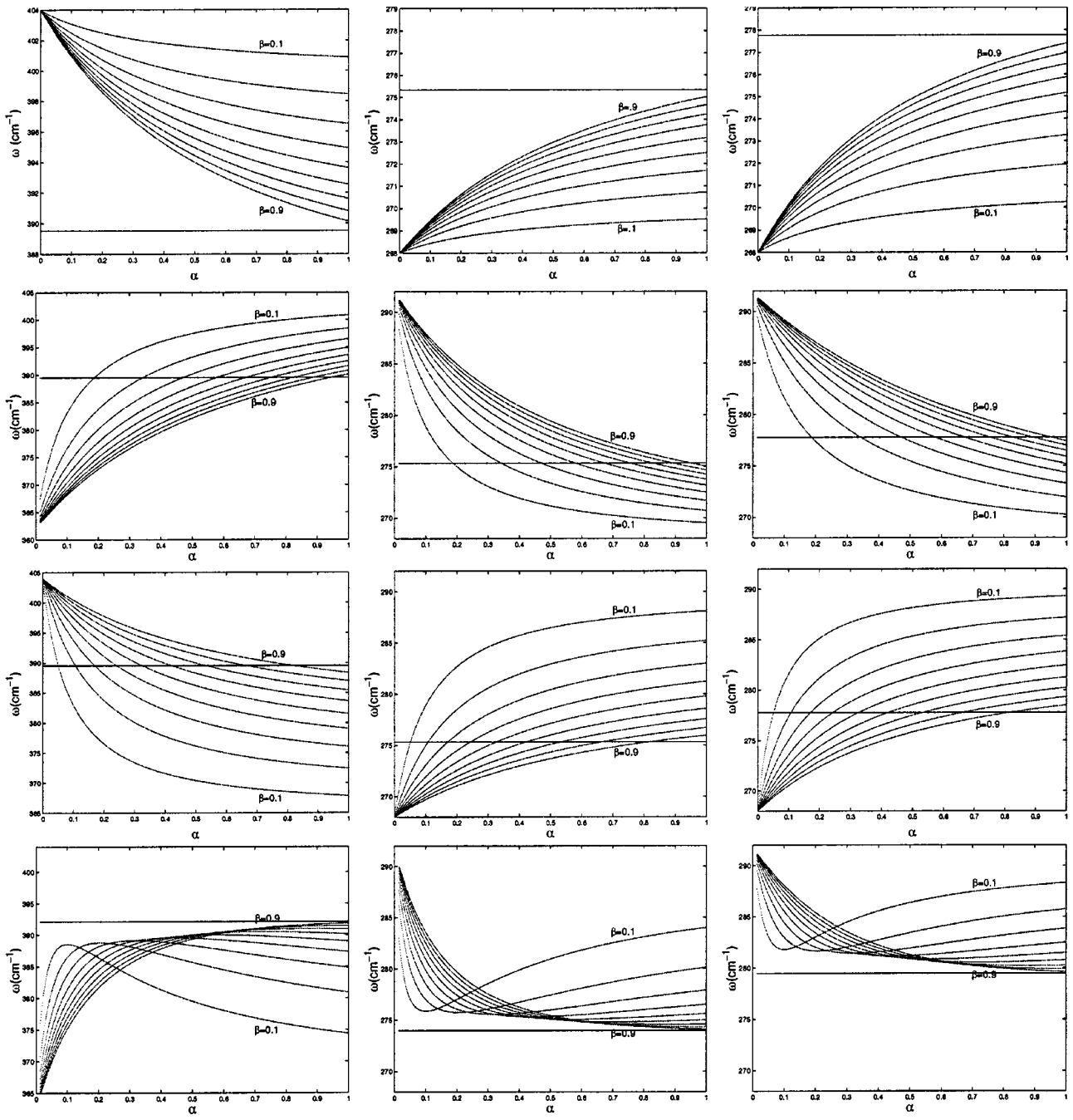

FIG. 2. Frequencies of the $(m,p)=(1,0)(1,1),(1,2),(2,4)$ SO modes (top to bottom) as a function of asymmetry using optically active host (left two panels, left for barrier-like modes, middle for dot-like modes), and a constant host dielectric constant (right panel). Note the different vertical scale for the barrier modes (left panel). The dot is spherical in the limit $\alpha,\beta\rightarrow 1$. The horizontal lines are the exact spherical results.

the other axis is then changed (hence, the multiple curves) until one approaches a sphere

$$\frac{y_0}{z_0}=\frac{\sqrt{\xi_1^2-b^2}}{\xi_1}=\beta. \tag{32}$$

Thus, the sphere is the limiting case of $\alpha=\beta=1$. The horizontal line is the frequency limit of a sphere and it is seen that the results for the ellipsoid do converge to that. The $l=1$ mode of the sphere has dot-like and barrier-like modes with frequencies 275.3 and 389.6 cm^{-1} for the active-host case, and a value of 277.8 cm^{-1} for the passive-host case. Thus, treating the host as a passive medium raises the frequency. We also observe that the numerical results for the ellipsoid are bounded between ω_{TO} and $[\epsilon(0)+\epsilon_D/\epsilon(\infty)+\epsilon_D]_{\mathrm{TO}}$ as found earlier. The shape dependence for spheroids was obtained by Comas *et al.*[8,9] They found that the behaviors are quite different for the prolate and oblate spheroids.

TABLE I. Gauss-Legendre quadrature.

Weights	Nodes
0.1012285363	±0.9602898565
0.2223810345	±0.7966664774
0.3137066459	±0.5255324099
0.3626837834	±0.1834346425

For example, for the $l=1$ and $l=2$ modes (corresponding to the same values of m for the ellipsoid but note that the second index for the spheroid is not the same as the second index for the ellipsoid), they found that the $[1,0]$ and $[2,1]$ modes (we use square brackets for the spheroidal modes) converge to the spherical results from earlier for the oblate spheroid but, for the prolate spheroid, this behavior is displayed by the $[1,1]$, $[2,1]$, and $[2,2]$ modes. For the ellipsoid, the $(1,1)$ and $(2,4)$ modes converge from above. In the spheroidal limit, we obtain that the frequency does not cross the spherical value (in agreement with Ref. 9), but it can do so for the ellipsoid.

We have repeated the calculations for higher ellipsoidal harmonics. Similar behavior to the $m=1$ modes is observed in the bounds and convergence to the sphere for, for example, the $(2,p)$ modes except for $(2,4)$. For the latter, we obtain the shape dependence given in Fig. 2. Indeed, a nonmonotonic shape dependence is obtained when one is away from the sphere and spheroid. Similar results had been reported for the spheroids[9] (for example, the $[2,2]$ mode of the oblate spheroid) but near the spherical limit. Hence, this is a distinctive behavior of the SO phonon mode frequencies in triaxial ellipsoidal QDs. Finally, the $l=2$ mode of the sphere has dot-like and barrier-like modes with frequencies 274.0 and 392.1 cm^{-1} for the active-host case, and a value of 279.5 cm^{-1} for the passive-host case. Overall, both the optically passive and active host models lead to dot-like modes that have similar shape dependence of the frequencies.

VI. CONCLUSIONS

The size independence of surface optical phonon mode frequencies in quantum dots has been shown analytically in order to reconcile apparently contradictory results in the literature. We have evaluated the eigenfrequencies and eigenmodes of surface optical phonons in ellipsoidal quantum dots using both an optically passive and active host. The degeneracies present in the spherical and spheroidal cases are removed. Mode frequencies both above and below the spherical values have been obtained. The $(2,4)$ mode is found to be the lowest mode displaying a nonmonotonic shape dependence of the frequency. An optically active host has little impact on the shape dependence of the dot-like modes and introduces additional barrier-like modes that generally have the opposite shape behaviour compared to the dot-like modes.

ACKNOWLEDGMENTS

This work was supported by an NSF CAREER award (NSF Grant No. 9984059) and a Balslev award (Denmark).

APPENDIX: GAUSS-LEGENDRE QUADRATURE

Gaussian quadratures are a simple yet powerful tool in numerical integration. Quadratures work by assigning weights to values of the function in the integrand at nodal points. Using this method the integration becomes a summation as given later

$$\int_a^b f(x)\,\partial x \simeq \sum_{k=1}^{N} w_k f(x_k). \tag{A1}$$

The placement of the nodal points is not arbitrary with locations determined by the number of nodes and the size of the interval. The result is a very good approximation.

Generally a Gauss-Laguerre quadrature would be used for integrations over $[0,\infty]$, however, in the case $a,b\approx\xi_0$ this method fails to accurately converge. Instead we used a Gauss-Legrendre quadrature over smaller subintervals with the transform $x=1/t$, as suggested by Garmier and Barriot,[16] to avoid further approximations. We chose to use an eight node quadrature due to its simplicity and smaller computational requirements. A listing of the node locations and weights can be found in Table I or for a more indepth understanding of quadratures the reader is suggested to Atkinson.[17]

The Gauss-Laguerre quadrature is defined over the interval $[-1,1]$. To accomodate other intervals we use a mapping $M:[-1,1]\rightarrow[u_n,u_{n+1}]$ as defined later

$$M(x)=\frac{a+b}{2}+\frac{x(b-a)}{2}, \tag{A2}$$

$$\int_a^b f(x)\,\partial x=\left(\frac{u_{n+1}-u_n}{2}\right)\times\int_{-1}^{1} f\left[\frac{(u_n+u_{n+1})+y(u_{n+1}-u_n)}{2}\right]\partial y. \tag{A3}$$

Thus, our algorithm becomes

$$(2m+1)E_m^p(\xi_0)\int_{\xi_0}^{\infty}\frac{\partial x}{\sqrt{(x^2-a^2)(x^2-b^2)}[E_m^p(x)]^2} \tag{A4}$$

$$=(2m+1)E_m^p(\xi_0)\times\sum_{i=1}^{N}\int_{u_i}^{u_{i+1}}\frac{t^{2m}\,\partial t}{\sqrt{(1-a^2t^2)(1-b^2t^2)}[E_m^p(t)]^2} \tag{A5}$$

$$= (2m+1)E_m^p(\xi_0)\sum_{i=1}^{N}\sum_{j=1}^{N'} w_j \frac{(u_{i,j}-u_{i,j+1})}{2} \times \frac{u_{i,j}^{2m}}{\sqrt{(1-a^2u_{i,j}^2)(1-b^2u_{i,j}^2)}[E_m^p(u_{i,j})]^2}, \quad \text{(A6)}$$

such that

$$\bigcup_{n=1}^{\infty}[u_n, u_{n+1}] = [0, \xi_0^{-1}], \quad \text{(A7)}$$

where $u_{i,j}$ denotes the jth node of the ith subinterval.

[1] R. Fuchs and K. L. Kliewer, Phys. Rev. **140**, A2076 (1965).
[2] R. Ruppin and R. Englman, Rep. Prog. Phys. **33**, 149 (1970).
[3] B. K. Ridley, *Electrons and Phonons in Semiconductor Multilayers* (Cambridge University Press, Cambridge, 1997).
[4] R. Englman and R. Ruppin, Phys. Rev. Lett. **16**, 898 (1966).
[5] R. Englman and R. Ruppin, J. Phys. C **1**, 614 (1968).
[6] Rajeev Gupta, Q. Xiong, G. D. Mahan, and P. C. Eklund, Nano Lett. **3**, 1745 (2003).
[7] P. A. Knipp and T. L. Reinecke, Phys. Rev. B **46**, 10310 (1992).
[8] F. Comas, C. Trallero-Giner, N. Studart, and G. E. Marques, Phys. Rev. B **65**, 073303 (2002).
[9] F. Comas, C. Trallero-Giner, N. Studart, and G. E. Marques, J. Phys.: Condens. Matter **14**, 6469 (2002).
[10] P. A. Knipp and T. L. Reinecke, Phys. Rev. B **45**, 9091 (1992).
[11] C. Kittel, *Introduction to Solid State Physics*, 7th ed. (Wiley, New York, 1996).
[12] P. M. Morse and H. Feshbach, *Methods of Theoretical Physics* (McGraw-Hill, New York, 1953).
[13] P. Moon and D. E. Spencer, *Field Theory Handbook* (Springer-Verlag, Berlin, 1961).
[14] E. T. Whittaker and G. N. Watson, *A Course on Modern Analysis* (Cambridge University Press, Cambridge, 1962).
[15] F. M. Arscott and I. M. Khabaza, *Tables of Lamé Polynomials* (Pergamon, New York, 1962).
[16] R. Garmier and J.-P. Barriot, Celest. Mech. Dyn. Astron. **79**, 235 (2001).
[17] K. E. Atkinson, *An Introduction to Numerical Analysis* (Wiley, New York, 1978).